

UPSIDE

Deliverable D4.4

Grant Agreement No.	101070931
Start date of Project	1 September 2022
Duration of the Project	48 months
Deliverable name	D4.4
Partner Leader	UF
Dissemination Level	PU

Status	Final
Version	V1.1
Submission Date	30-11-2025

Author(s)	Prof. Dr. Máté Döbrössy (UF)
Co-author(s)	Lisa Ratz (UF)

UPSIDE project has received funding from the European Union's Horizon Europe EIC-PATHFINDER programme under grant agreement No 101070931.





European
Innovation
Council



Funded by the European Union. Views and opinions expressed are however those of the author(s) only and do not necessarily reflect those of the European Union or EISMEA. Neither the European Union nor the granting authority can be held responsible for them

PU=Public, SEN=Confidential, only for members of the consortium (including the Commission Services), CI=Classified, as referred to in Commission Decision 2001/844/EC.

House Style

	Red RGB	Green RGB	Blue RGB	HEX
				
Pink	247	181	192	#F7B5C0
Grey	161	161	161	#A1A1A1
Blue	41	171	226	#29ABE2
 <p>THE USE OF THE EU EMBLEM IN THE CONTEXT OF EU PROGRAMMES 2021-2027 LINK In addition to the obligations set out in Article 17, communication and dissemination activities as well as infrastructure, equipment or major results funded under EIC actions must also display the following special logo:</p>				
 				
EU corporate blue	0	51	153	#003399
Yellow	255	204	0	#FFCC00

Authors, Co-authors and contributors

Author	Organization	E-mail
Prof. Dr. Máté Döbrössy	UF	mate.dobrossy@uniklinik-freiburg.de
Lisa Ratz	UF	lisa.ratz@uniklinik-freiburg.de

Quality Control

Author	Name	Date
WP leader	Prof. Dr. Máté Döbrössy	27-11-2025
Internal reviewer	Prof Tiago Costa	29-11-2025
Coordinator	Prof Tiago Costa	29-11-2025

History of Changes

Version	Change made	Date
V1.0	First draft	27-11-2025
V1.1	Final version	29-11-2025

Table of Contents

Executive Summary.....	4
1. Introduction	5
2. Methods and Results	8
2.1 Electrophysiological measurements with the eREC ₆₄ device.....	8
2.1.1. Study design	8
2.1.2. Behavior and corticosterone measurements	10
2.2. FUS stimulation in awake freely moving rats.....	11
2.2.1. Validation of targeting accuracy via BBB opening.....	11
2.2.2. chronic eFUS stimulation and Fiber Photometry measurements	13
3. Conclusions	19
Annex 1: MATLAB script.....	21
4. References	22

List of Figures:

Figure 1 Study design eREC64 recordings in an animal model of depression.	8
Figure 2 Surgery chronic eREC64 implantation.	9
Figure 3 Fig.3. Behaviour results Forced swim test (FST)	10
Figure 4 Preliminary results of corticosterone levels in feces	11
Figure 5 Visualisation of focal spot through BBB opening using SonoVue microbubbles © and eFUS stimulator	12
Figure 6 Chronic implantation of the epidural Focused Ultrasound chip (eFUS).	13
Figure 7 Scan of multiple locations in animal 1 implanted with chip R5C4 and stimulated with parameter set 1 at 8 mm depth.....	15
Figure 8 Delta F/F signal separated by stimulation repetition at one location with parameter set 1 in all 3 animals	16
Figure 9 Stimulation of animal 1 with chip R5C4 at AP 0/ML -0.6/DV-8 mm with parameter set 4	17
Figure 10 Iba 1 staining to check for tissue damage or inflammation at the stimulation site in an animal implanted with a Dummy chip (A),as well as the 3 real chips (B-D)	18

List of Tables:

Table 1 Animal numbers eREC64 recordings	10
Table 2 Tested conditions for BBB opening as target validation	12
Table 3 Overview of tested FUS parameters	15

Abbreviations

ACC	anterior cingulate cortex
BBB	blood brain barrier
DBS	Deep Brain Stimulation
DC	duty cycle
EB	Evans blue
EBI	Epidural Brain interface
ECoG	electrocorticography electrodes
EEG	Elektroenzephalographie
eFUS	epidural Focused Ultrasound
FCM	Fecal corticosterone metabolites
FP	Fiber Photometry
FSL	Flinders sensitive Line
FST	Forced swim test
LCP	Liquid Crystalline Polymer
MB	Microbubbles
mfb/ MFB	medial forebrain bundle (small letters refer to rats, capitals refer to humans)
MRI	magnetic resonance imaging
NAC	nucleus accumbens
PCB	Printed Circuit Board
PNP	Peak negative pressure
PNP	peak negative pressure
PRF	pulse repetition frequency
SD	Sprague Dawley
TUD	TU Delft
vmPFC	ventromedial pre-frontal cortex
VTA	ventral tegmental area
WP	Work Package

Executive Summary

Document D4.4. summarizes the current state of progress in our on-going efforts to validate *in vivo* - in awake and freely moving animals - two separate key functions of the future epidural brain interface (EBI) device: First, the *electrophysiological recording/* monitoring of neuronal activity using 32 and 64-channel grid/ electrocorticography electrodes (ECoG); and second, the *epidural focus ultrasound (eFUS)* chip's capacity for neuromodulation evidenced as its capacity to induce distal neurotransmitter release.

Identifying biomarkers are key for the development of closed-loop stimulation options, as well as for monitoring disease dynamics and brain states associated with susceptibility to anxiety and depression episodes. The current document describes the use of the FSL rodent depression model and control animals (SD) for the *in vivo* validation of the implanted cortical electrode. The 64 channel grid ECoG electrodes were manufactured by our partners in Ghent and implanted into and tested in the experimental animals in Freiburg (to date: FSL, n=9; SD, n=3). The collected electrophysiological data was transferred to and analyzed by the team at Newronika. Baseline/ resting state recordings were made of pre-frontal cortical neural activity across the experimental groups; an acute, high-stress condition was introduced to maximize the contrast between the idle vs stress state, in order to assess state specific differences in brain oscillation in the control and disease model. The experimental groups need to be enlarged, but preliminary analysis indicates that condition-dependent differences across the FSL and the control animals were noted both at the power spectral density and high beta and high gamma bands. A full report on the outcome can be found in the Newronika report D5.1.

The second part of the document describes the on-going *in vivo* validation of the eFUS chip, and in particular the capacity to modulate dopamine release in the nucleus accumbens following targeting of the medial forebrain bundle/ ventral tegmental area. Changes in the chip design, the testing protocol, the data collection, the development of analysis pipelines, overcoming emerging challenges, and the preliminary *in vivo* data from the first three fully implanted awake and longitudinally tested animals are presented.

D4.4 has been delayed due to the late supply of the first batch of fully implantable eFUS chips. Many more chips will be needed for *in vivo* testing to comprehensively assess the chip's capacity to modulate physiological process/ network activity. Additional ECoG electrodes will also be need to increase the experimental group sizes. The lateness of this Deliverable has no significant impact on the eventual submission of future Deliverables/ Milestones from WP4.

1. Introduction

D4.4. ePhys Biomarker detection and impact of FUS stimulation on neurotransmitter release

The UPSIDE project proposes an Epidural Brain Interface (EBI) device with dual functions combining an *epidural focused ultrasound* system for steerable, multi-site neural stimulation (eFUS) and a high spatial-temporal resolution device for *neural activity recording* from the cortex (eREC). As the project stands, the two functions (the stimulation and recording capacities) are encapsulated by two independent devices. Deliverable D4.4 goes towards the separate *in vivo* testing of the two devices and addresses the independent features of the future integrated EBI device.

i.) Electrophysiological biomarker detection in the rodent model. The electrophysiological recording capacity will contribute to the EBI's overall function by monitoring cortical network activity essential for identification of biomarkers signaling different stages in the disease dynamics (e.g. asymptomatic, symptomatic, remission, etc). Biomarkers are reliable, consistently measurable biological indicators that are predictors of susceptibility to or associated with an ongoing (pathological) condition or diseases. Biomarkers used for depression diagnosis can be neurochemical, biochemical, neuroimaging, speech or EEG/ electrophysiology based. Rhythmic voltage fluctuations emerge through synchronized neuronal electrical activity, or oscillations, within neuronal networks. The oscillations, or brain rhythms present in both cortical and subcortical areas, are temporally and spatially synchronized fluctuations in neuronal excitability and specific activities are associated with diverse functions and cognitive phenomena, including language and brain states in health and diseases^{1,2}. Identifying and integrating biologically meaningful, electrophysiological biomarkers into the functioning of the future EBI would enhance its therapeutic value in several ways: it would permit the acute/ chronic monitoring of the disease state (as reflected by changes in neural network activity), as well as the impact of the neurostimulation; understanding biomarkers would also permit the development of closed-loop/ adaptive stimulation, activating the stimulation function when needed (and according to the parameters and target site needed), and not on a permanent basis.

Brain waves divided into different groups according to their frequency ranges:

Delta	Theta	Alpha	Beta	Gamma
0.5-4 Hz	4-8 Hz	8-12 Hz	12-30 Hz	30-150 Hz

Traditionally, alpha (8-12 Hz) and beta (16-30 Hz) oscillations have been studied as biomarkers in the context of psychiatric and neurological disorders and there is growing evidence that gamma rhythms (low gamma 30-45 Hz, high gamma 60-100 Hz) could be used as a biomarker for depression too. Diverse EEG biomarkers at multiple cortical regions implicating different brain networks have been associated with clinical depression (for review see³). Indeed, EEG biomarkers from depression patients from all five major frequency ranges have been described, underscoring i.) the symptomatically and biologically heterogenous nature of major depressive disorder is also reflected in the diversity of biomarkers; and ii.) necessitating in the future to individually assess patients and identify person-specific biomarkers.

Our research, along with multiple other labs internationally, uses the Flinders Sensitive Line (FSL) rat model of depression. The animal model has been described in our previous reports and many peer reviewed publications⁴⁻⁶. Electrophysiologically orientated data from other groups using the FSL have

reported – compared to the control animals - decreased power of neuronal oscillations in the alpha (8-12 Hz), beta (12-30 Hz) and low gamma range (30-45 Hz) in the ventromedial prefrontal cortex (vmPFC), nucleus accumbens (NAc) and the ventral tegmental area (VTA)⁷⁻¹⁰. For example, Voget and colleagues (2015) compared LFP recordings from FSL and control rats and showed that resting state alpha, beta and low gamma oscillatory activities were significantly lower in the vmPFC and NAc of FSL rats compared to controls. Others highlighted that both high and low gamma oscillations were significantly decreased in the VTA of FSL rats compared to control⁸. Our group in Freiburg looked at the differences in electrophysiological biomarkers across the FSL and the control animals both at resting state and at post-stimulation conditions, using medial forebrain bundle DBS as the stimulation modality. Animals were anesthetized during these studies. Resting state recordings, as well as stimulation induced responses, have identified divergent neuronal oscillations across FSL and SD rats. Particularly, beta oscillatory activity, as well as low-gamma activity, in the vmPFC were significantly reduced in the experimental depression model¹¹. Additional earlier studies (similarly in anesthetized animals) have confirmed resting-state and stimulation induced differences between FSL and control animals in the theta, beta and gamma range (manuscript in preparation). The role of beta oscillatory activity has mainly been discussed in the context of Parkinson's disease, where the dopamine level in the basal ganglia is inversely correlated to beta oscillatory activity¹². Others have confirmed that cortical beta oscillations across the neocortex and basal ganglia map onto shared functional and structural networks that show significant positive correlations with dopamine receptors, and are modulated by dopamine¹³. Clinical literature associates alterations in beta oscillations in the PFC with deficits in working memory, increased anxiety levels and impaired executive control of thought, symptoms present in – but not exclusive to – depression^{14,15}.

The first part of the current D4.4 report describes our ongoing effort to identify biomarkers capable of distinguishing the FSLs from the control animals. The study design (see Methods and Results section for details) included FSL and control animals, and repeated and longitudinal recording of bilateral/ prefrontal cortical neural activity, under multiple conditions including resting-state, acute anxiogenic/ stressful, and post-recovery conditions. The hypothesis was that electrophysiological measurements across the experimental groups under the highly contrasting conditions would increase the chances of detecting experimental group and condition specific biomarkers. Stress plays a critical role in the development of depressive symptoms, both clinically and in animal models. The FSL model, characterized by increased stress vulnerability and depressive-like behavior, provides a valuable framework for analyzing the relationship between stress and depression, including the reaction and adaptation to and management of stress. The work was done in awake, freely moving animals using the implanted 32-channel ECoG electrode manufactured and supplied by our partners in Ghent. Full descriptions of the device can be seen in previously submitted documents. The electrophysiological data collected was transferred to and analyzed by Newronika. A report on the on-going and partial data analysis, concerning the data collected in the study described in this deliverable, is available in their recent report (D5.1).

ii.) Neurophysiological impact of eFUS stimulation on neurotransmitter release. The EBI device will have neuromodulatory capacity achieved via the epidural chip emitting low-intensity focused ultrasound (eFUS), including high spatial/ temporal resolution targeting and beam steering feature. The stimulation characteristics of the eFUS have been demonstrated *in vitro* (see previous report(s) from TUD) and the initial and preliminary *in vivo* testing strategy in anesthetized animals has also been described previously (Freiburg D4.3).

The second part of the current document provides an update of our work since D4.3, and focuses on the emerging and on-going *in vivo* data obtained from awake, freely moving animals. eFUS stimulation of the

medial forebrain bundle (mfb) / VTA is expected to modulate the neurotransmitter systems passing through the fiber bundles which we aim to monitor using Fiber Photometry (FP), an innovative neurotransmitter/ neuronal activity monitoring technique. FP is a state-of-the-art method measuring neuronal population bulk activity changes or the extracellular availability of key neurotransmitter system traversing the mfb, like dopamine, noradrenaline or glutamate¹⁶⁻¹⁹. FP offers several advantages over more traditional approaches such as dialysis or fast scanning cyclic voltammetry: i.) the neurotransmitters can be defined very specifically, and electrochemically inert substances like glutamate can also be detected; and ii.) chronic in vivo repeated measurements over a period of up to about 2 months can be performed without loss of signal. Using FP, in the past we have demonstrated that mfb DBS induces acute and enduring release of dopamine and noradrenalin in forebrain structures, e.g. prefrontal cortex and nucleus accumbens; that the release patterns are stimulation paradigm dependent; and that stimulation has differential effects on the depression model vs controls. Past results confirmed that modulation of monoamine release in key structures on the reward pathway are likely to be involved in the antidepressant mechanisms of mfb DBS²⁰⁻²⁴.

D4.4 revisits and further analyses data from the eFUS effects in the anesthetized animals. Furthermore, we describe novel data from the first three awake, and freely moving animals with the fully implantable version of the eFUS chip, including the stimulation paradigms, data collection and MATLAB based data analysis protocols, and the results of the on-going assessment of stimulation induced physiological effects.

UNDER REVIEW

2. Methods and Results

2.1 Electrophysiological measurements with the eREC₆₄ device

2.1.1. Study design

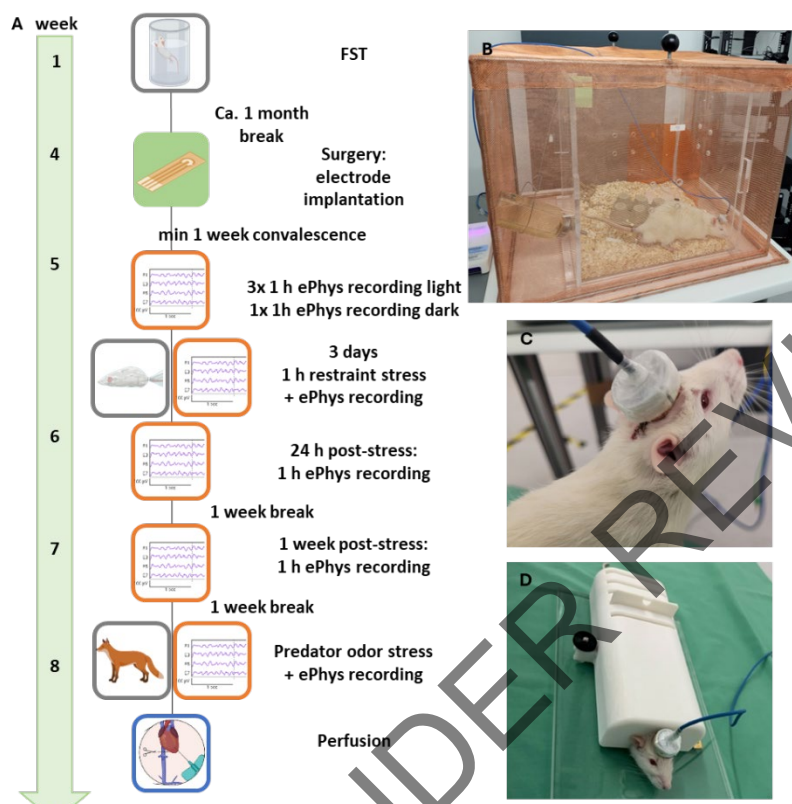


Figure 1 Study design eREC₆₄ recordings in an animal model of depression.

A Timeline **B** Recording of animal in homecage (ePhys recording light) inside a Faraday cage. **C** Headstage of animal connected to the Open ePhys © system. **D** Restrained animal for immobility stressor

The timeline for the recordings aiming to detect potential electrophysiological biomarkers in the Flinders Sensitive Line (FSL) as an animal model of depression is shown in Figure 1 A. All animals initially underwent the Forced Swim Test (FST). The test measures the depression-like phenotype of the animals by assessing hopelessness and passive stress-coping in the face of an inescapable situation. This is indicated by the time they remain immobile when placed for 7 minutes in a water-filled tank where they cannot reach the bottom.

Classically, not all FSL animals show the depressive phenotype to the same extent, and the most mobile animals are often excluded from behavioural tests. In our case, all animals were implanted with the eREC₆₄ device to detect differences in the severity of a potential biomarker even within the model. To ensure the experiments were not affected by the

FST as an acute stressor, the eREC₆₄ device was implanted one month later.

The surgery for the chronic implantation is shown in Figure 2. A 2.5 × 3 mm craniotomy was drilled above the anterior cingulate cortex (ACC) and prefrontal cortex (PFC; exact placement shown in Fig. 2F & G). The eREC₆₄ probe was placed on top of the dura (Fig. 2 E) and sealed with the explanted bone and dental cement, and the SPI headstage from Open Ephys © was fixed in place with a custom-designed 3D-printed headpiece. The connector was protected from dust and liquid with a small cap while the animal was in the cage.

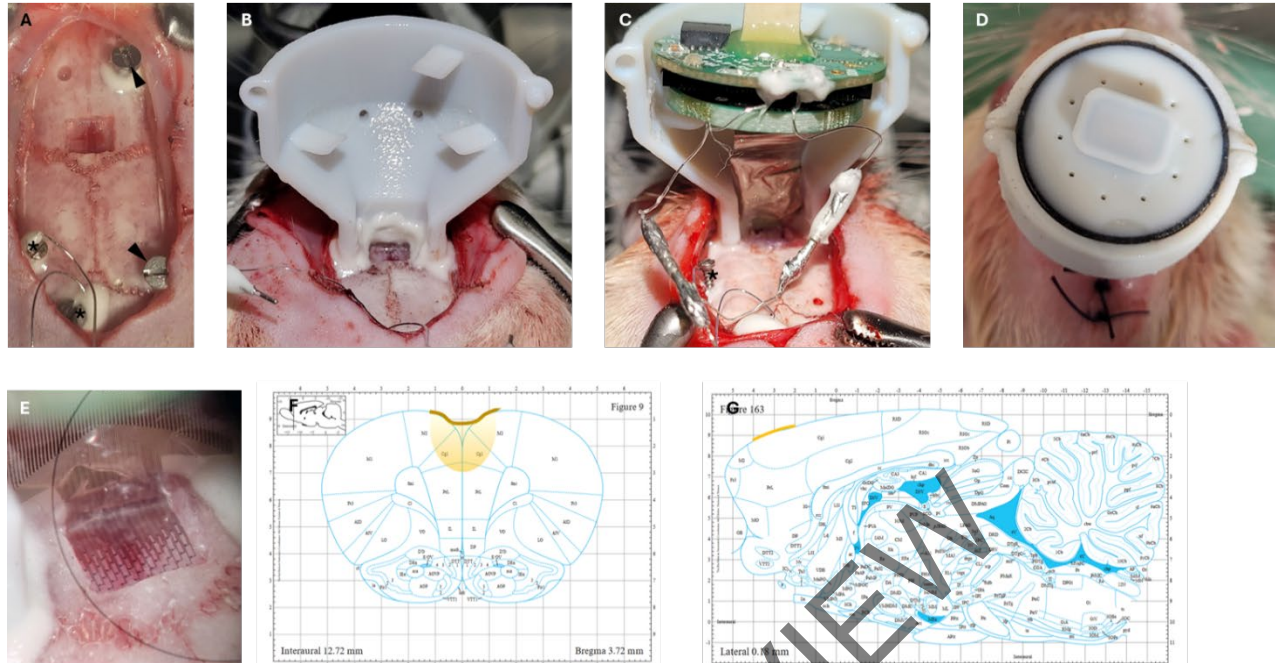


Figure 2 Surgery chronic eREC64 implantation. **A** Craniotomy at AP +1.9-4.0mm /ML +/- 1.4mm ground and reference screw marked with asteriks (*) Anchor screws marked with black arrow **B** 3D printed backpiece of headpiece **C** Implanted open ePhys SPI headstage and UPSIDE eREC probe connected with ground and referce screw (*) **D** Complete headpiece with small cap to protect connector **E** 64 electrode probe placed in craniotomy **F** ML placement of electordes above anterior cingulate cortex marked in yellow, recoding depth indicated **G** AP placement of electrode marked in yellow

After surgery, the animals were given at least one week to recover before the first electrophysiological recordings were conducted. The ACC activity was recorded for one hour during the light phase (resting time for nocturnal animals) on three days in the animals' home cage and once during the dark (active) phase. The animals were allowed to freely roam the cage, drink, eat, and sleep. The recording quality was improved through a Faraday cage (Fig. 1B). The collected data were transferred to our UPSIDE partner Newronika © for analysis to detect any baseline/ resting state differences in brain oscillations between FSLs and SDs.

Because the FSL model differs the most in their stress-coping behaviour (see FST), two different stressors were included following the home-cage recordings to assess a potential stress-evoked biomarker. The initial stressor used was "restraint stress". The animals were immobilized for on three consecutive days 1 hour each in a custom restrainer that leaves the head and implant free to record during the stressor. At 24 hours and 1 week after the final stress session, the animals were recorded again to assess a potential washout of the biomarker. Two weeks after the immobility stress, the animals were placed for 10 minutes in a separate cage which contained a neutral odor (water). The following day this was repeated a predator odor (bobcat urine). The anxiety-related stress reaction is inherent to the animals and has been shown to reveal differences between stress-resilient and stress-susceptible animals in a PTSD model²⁵. At the end of the study, animals were perfused for further histological analysis of the brain.

In order to learn to correlate any ePhys biomarker with the animals individual stress reactivity, fecal corticosterone metabolites (FCMs) were measured in feces collected over the course of a baseline days as well as during and after the restraint-stress immobility conditions. Corticosterone—the primary stress hormone in rodents—is metabolized and excreted in feces approximately 8 hours after secretion. FCM levels were measured using a Corticosterone ELISA from Enzo Life Sciences ©.

Table 1 Animal numbers eREC64 recordings

SD=Sprague Dawley FSL= Flinders Sensitive Line

experimental groups	SD	FSL	total #
♀	2 (+3)	5 (+2)	7
♂	3 (+2)	4 (+2)	7
total #	5 (+5)	9 (+4)	14 (+9)

At the time of this deliverable report, a total of 14 animals (equal numbers of males and females) had been recorded from, including 5 SDs and 9 FSLs (Table 1). To ensure adequate statistical power, the number of animals will be increased to at least 10 SDs and 10 FSLs by the end of the project. Additional FSLs will be included to ensure a representative range of the depressive phenotype.

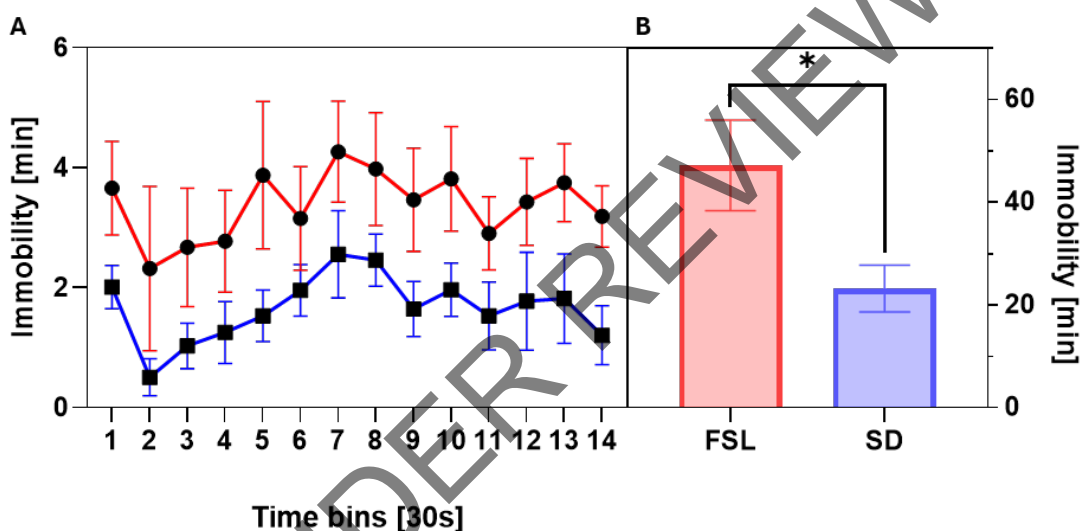


Figure 3 Fig.3. Behaviour results Forced swim test (FST) A Immobility throughout the 7 min test period, shown in 30 s timebins **B** overall immobility; SD=Sprague Dawley, FSL= Flinders Sensitive Line

2.1.2. Behavior and corticosterone measurements

In addition to the main results concerning potential electrophysiological biomarkers (described in great detail in report D5.1 from Newronika), the behavioural tests and corticosterone measurements around the immobility stress are shown in Figures 3 and 4. In the behavioural test, the FSLs showed greater immobility throughout the test and overall, as expected. This includes animals already part of the electrophysiology dataset as well as animals that have undergone the FST but are not yet implanted.

The preliminary results regarding corticosterone levels in FSLs and their changes in response to immobility stress are shown in Figure 4. Due to the limited sample size (n=3 for both FSLs and SDs), the results are not significant but indicate that FSL animals tend to show overall higher corticosterone levels, with an earlier daily peak (around 20–22 h). Additional analysis is being done at the time of writing of this report. When individual animals are normalized to their own baseline FCM levels, the stress effects (measured in feces collected 7-9 h after the start of the stressor) increase across the stress days. In comparison, SDs

show lower baseline levels but a higher proportional stress induced increase, which in some animals is already visible on day 2.

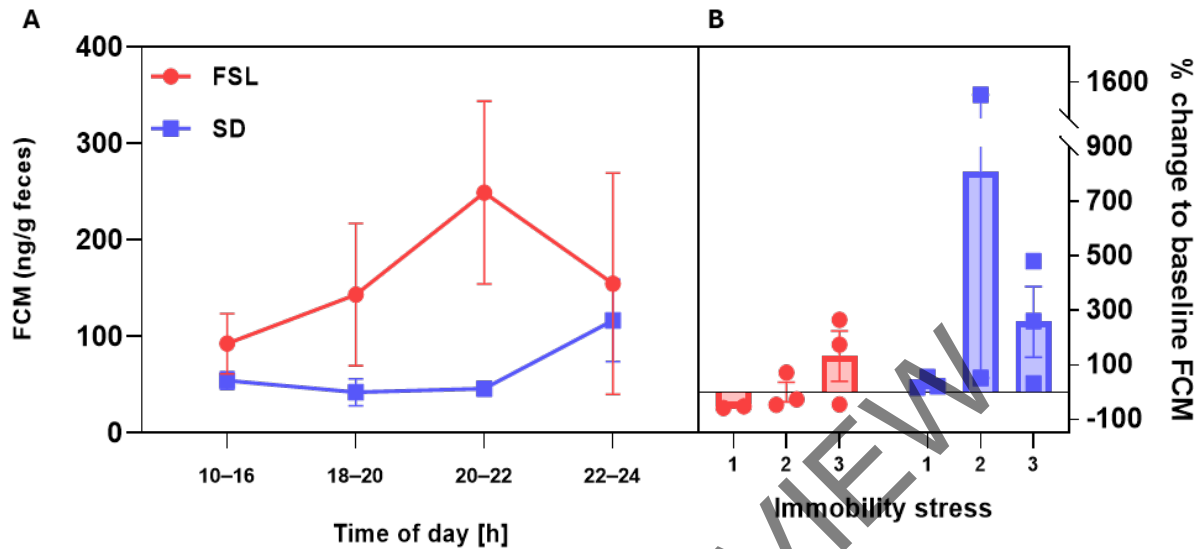


Figure 4 Preliminary results of corticosterone levels in feces **A** of naive animals **B** and after immobility stress day 1,2 and 3; SD= Sprague Dawley, FSL= Flinders Sensitive Line, FCM = Fecal corticosterone metabolites

2.2. FUS stimulation in awake freely moving rats

2.2.1. Validation of targeting accuracy via BBB opening

As the chip is currently not MRI-compatible, targeting accuracy was assessed by opening the blood–brain barrier (BBB) using microbubbles. The eFUS chip was implanted under anesthesia, and 5×10^8 SonoVue © microbubbles as well as 4–5% Evans Blue dye was injected into the tail vein of the animal. Three to five targets in one animal were stimulated using the same set of parameters for up to 2 minutes. Through BBB opening at the focal spot, the dye was able to extravasate into the surrounding tissue. The animals were sacrificed 2 hours later and prepared for fluorescence microscopy to detect even small amounts of dye. The tested conditions are shown in Table 2.

Table 2 Tested conditions for BBB opening as target validation PRF = Pulse repetition frequency, DC= Duty cycle, PNP= Peak negative pressure, MB= Microbubbles, bw= body weight, EB= Evans blue

condition	PRF [kHz]	DC [%]	PNP @8mm [MPa]	SD [s]	MB conc [MB/kg bw]	EB conc [%]	target depth [mm]
1	1	10	0,5	5 x 120	4 x 10 ⁷	4	-1,5 / -8
2	1	50	0,5	5x 120	5 x 10 ⁸	4	-1,5 / -8
3	1	10	0,5	5x 120	5 x 10 ⁸	4	-1,5 / -8
4	0,01	30	0,4	30, 60, 120	5 x 10 ⁸	5	-5
5	0,01	10	0,38	3x 120	5 x 10 ⁸	5	-5

Figure 5 shows the assessment targeting accuracy of the chip through microbubble induced BBB opening. The stimulation parameters tested are listed in Table 2. The most promising results were obtained with parameter sets 2 (Fig. 5 B–C) and 5 (Fig. 5 E), which may indicate that longer pulse lengths

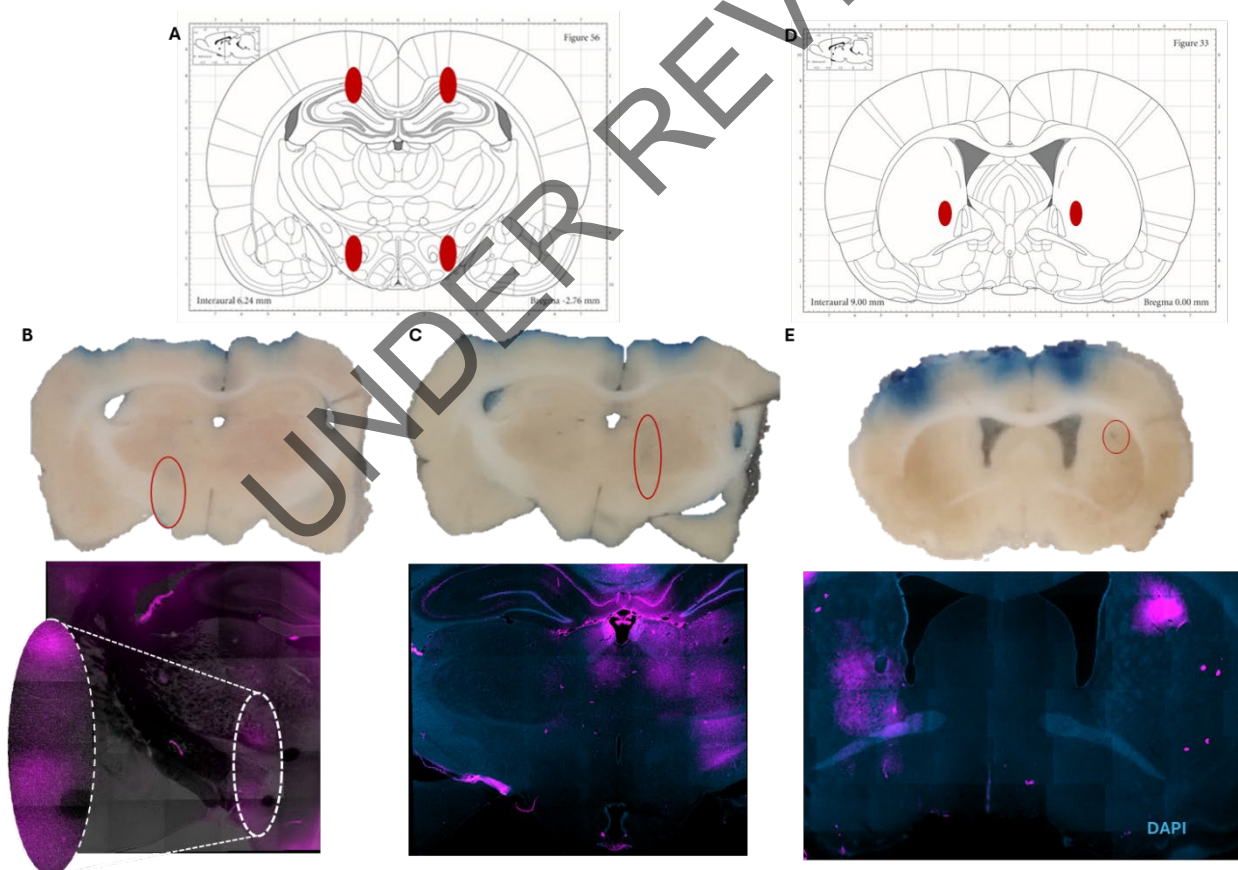


Figure 5 Visualisation of focal spot through BBB opening using SonoVue microbubbles © and eFUS stimulator A stimulation targets in conditions 1-3 at 1.5 and 8 mm depth. B Stimulation condition 2, Evans blue seen in frozen brain (top) and fluorescent signal (bottom) in left mfb (red circle top, white circle bottom) C condition 2 targeting right mfb in the same animal D stimulation targets condition 4 and 5 E Effects of stimulation condition 5, no Evans blue visible in frozen brain but fluorescent signal

combined with lower PRFs allow the use of lower duty cycles. However, these findings are currently based on only one animal per condition.

In all cases, Evans Blue dye was barely or not at all visible to the naked eye (top panels B, C, E). The drilling of the craniotomy, the fixation of the chip with screws, and potential heating during prolonged high-intensity stimulation produced off-target cortical BBB opening that appeared independent of stimulation. As a result, dye extravasation specifically due to cortical stimulation in condition 2 was difficult to distinguish from background signal.

Generally, most likely due to the limited half-life of microbubbles and the decrease in focal pressure when the ultrasound beam is steered, the strongest signal was consistently observed at the stimulation location perpendicular to the center of the chip—the first position stimulated. Fluorescence microscopy confirmed Evans Blue extravasation at this site, suggesting that perpendicular stimulation is mostly spatially accurate in all axes. This also indicates that the stereotactic implantation was precise and the chip was not tilted. On the contralateral hemisphere, the focal spot appeared either rather broad (Fig. 5 C) or concentrated around a blood vessel (Fig. 5 E). In both cases, the BBB opening appeared to be slightly more lateral or ventral than intended.

These results suggest that perpendicular stimulation is accurate, but that the chip's steering capability remains useful for identifying the stimulation location producing the strongest effect within the target region.

2.2.2. chronic eFUS stimulation and Fiber Photometry measurements

To avoid any masking of stimulation effects due to anaesthesia, recent stimulation tests with the eFUS chip were performed in awake, freely moving animals chronically implanted with the device. The surgery and recording setup are shown in Figure 6. At least one month before the chip implantation three male SD animals (~16 weeks old) were unilaterally injected with the dopamine sensor GRABDA2m²⁶ into the left NAc shell to allow sufficient viral expression (see Fig. 6 F & G).

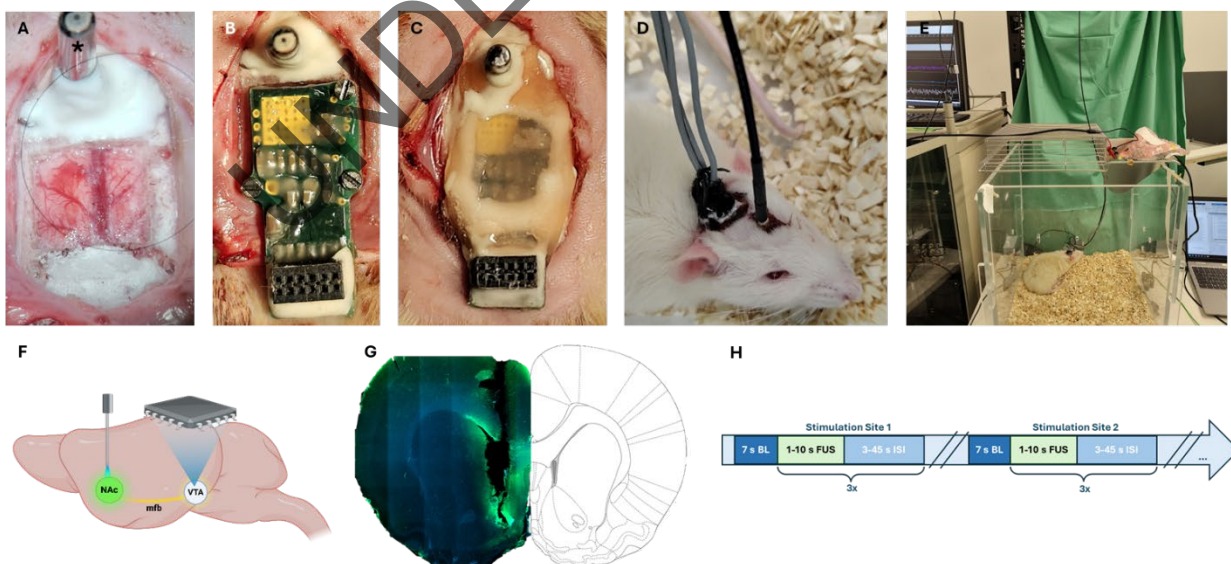


Figure 6 Chronic implantation of the epidural Focused Ultrasound chip (eFUS). **A** Craniotomy around left VTA and implanted optic fiber (*) in left Nac for Fiber photometry **B** eFUS chip fixed with screws **C** eFUS chip fixed with dental cement **D** animal connected to FP recording and eFUS stimulation system **E** FUS stim setup **F** diagram of FUS stimulation of VTA and expected dopamine release in the NAC measured with FP **G** exemplary placement of optic fibre and dopamine sensor in left Nac

To implant the chip on top of the dura, a 7.5 × 8 mm craniotomy was drilled around the left VTA (AP-5.2/ML 0.7mm/DV -8 mm; Fig. 6A). An optic fibre was implanted in the left NAc, at the site of dopamine sensor expression, to measure neurotransmitter changes. The chip was fixed to the skull with screws and sealed with Kwik-Sil © and dental cement to secure the implant, close the craniotomy, and protect the chip from moisture or from the tissue. The centre of the chip was positioned perpendicular to the VTA to maximize acoustic pressure (schematic in Fig. 6F).

Once the animals had sufficient recovery time, fiber photometry recordings during eFUS stimulation were performed in a separate cage. To ensure optimal chip performance, the cable length was limited to 45 cm, and only the ipsilateral hemisphere was stimulated.

In the first phase of the experiment, the chip's beam-steering capability was used to "scan" the stimulation site with a single set of parameters to detect changes in dopamine release elicited by eFUS stimulation.

Using the GUI provided by TU Delft, the focal spot was positioned perpendicular to the centre of the chip at the depth of the VTA, at coordinates AP/ML/DV: 0/0/-8 mm. Each location was stimulated 3 times before the chip automatically steered to the next position. In total, 9–12 locations within one plane were stimulated, covering ±1 mm in AP (1 mm steps) and ±0.9 mm in DV (0.3 mm steps). For some parameter sets, multiple planes were tested (DV -8 ± 1 mm). On the following day, a new parameter set was tested, as the optimal conditions for robust stimulation effects were not yet known. The tested parameters are shown in Table 3 and the stimulation pattern is depicted in fig. 6 H.

The fiber photometry data from each stimulation site was analyzed using pMAT v1.2 (The Barker Lab, Philadelphia, PA, USA) and a custom-made MATLAB R2025b (The MathWorks Inc., Natick, MA, USA) script (see Annex 1). The raw GFP signal (465 nm, F₄₆₅) from the GRABDA2m dopamine sensor activity was fitted to the the isobestic signal (405 nm, F₄₀₅) in order to obtain the corresponding dopamine fluorescence (DeltaF/F).

$$\frac{\Delta F}{F} = \frac{F_{465} - F_{405}}{F_{405}}$$

The data can then be normalized to the event related baseline, this encompassed here the 7 s before the first stimulation of each site with one parameter. This results in the robust event related z-score:

$$\frac{\Delta F}{F} z - score(i) = \frac{\frac{\Delta F}{F} FUS stimulation (i) - median(\frac{\Delta F}{F} baseline)}{median absolute deviation (MAD) of baseline}$$

Table 3 Overview of tested FUS parameters

name	frequency	pulse repetition frequency	duty cycle	Peak negative pressure			sonication duration	inter stimulus intervall	# Bursts
Abb.	f	PRF	DC	PNP [Mpa]			SD	ISI	
	[MHz]	[kHz]	[%]	R5C1	R5C2	R5C4	[s]	[s]	
1	4	0,0025	20	0,37	0,12	0,29	1	45	3
2	4	0,0025	5	0,37	0,12	0,29	5	45	3
3	4	0,02	3			0,29	10	30	3
4	4	1	36			0,29	0,5	30	3
5	4	1,5	45			0,14	0,2	1,8	2* 3
6	4	0,2	4			0,29	1	3	5

In these first three chronically implanted animals, none progressed to the next phase. Two animals lost their implants before all parameters could be tested, and the chip in the third animal experienced a short circuit, requiring premature termination of the experiment. In total these first chips were successfully implanted for 3-7 weeks.

In future animals, this first phase will be shortened based on the collected data, and stimulation will focus on the most promising target location using a systematic range of pulse repetition frequency (PRF), duty cycles, and intensities.

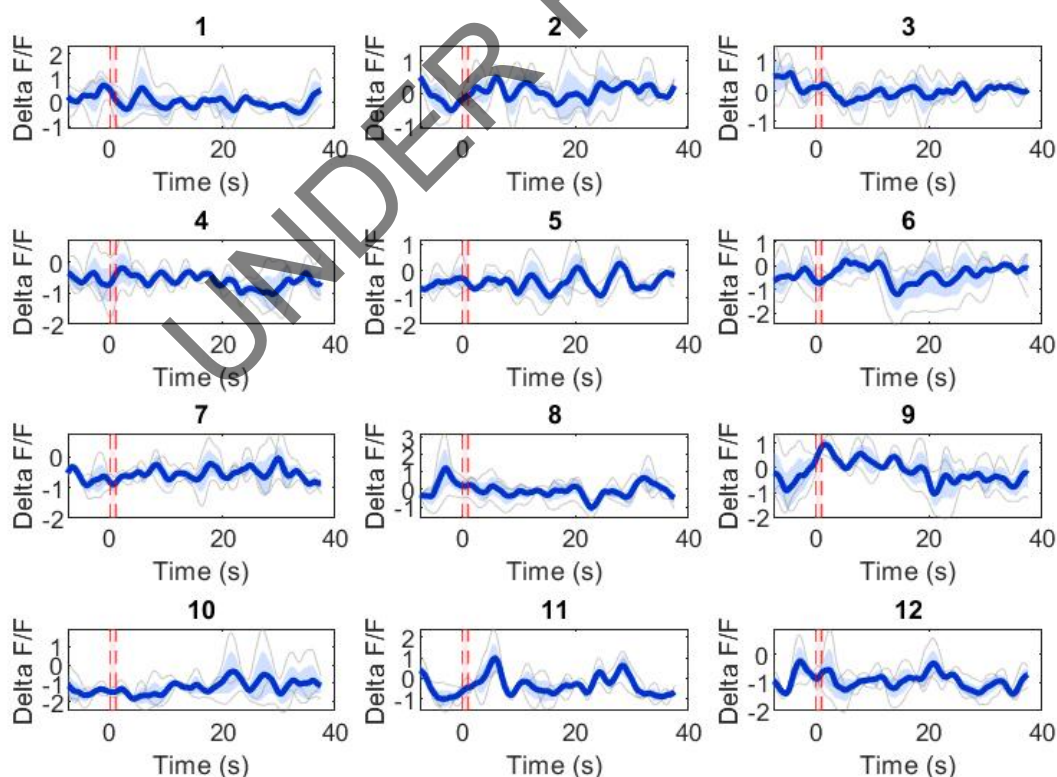


Figure 7 Scan of multiple locations in animal 1 implanted with chip R5C4 and stimulated with parameter set 1 at 8 mm depth. The stimulation duration is marked in red.

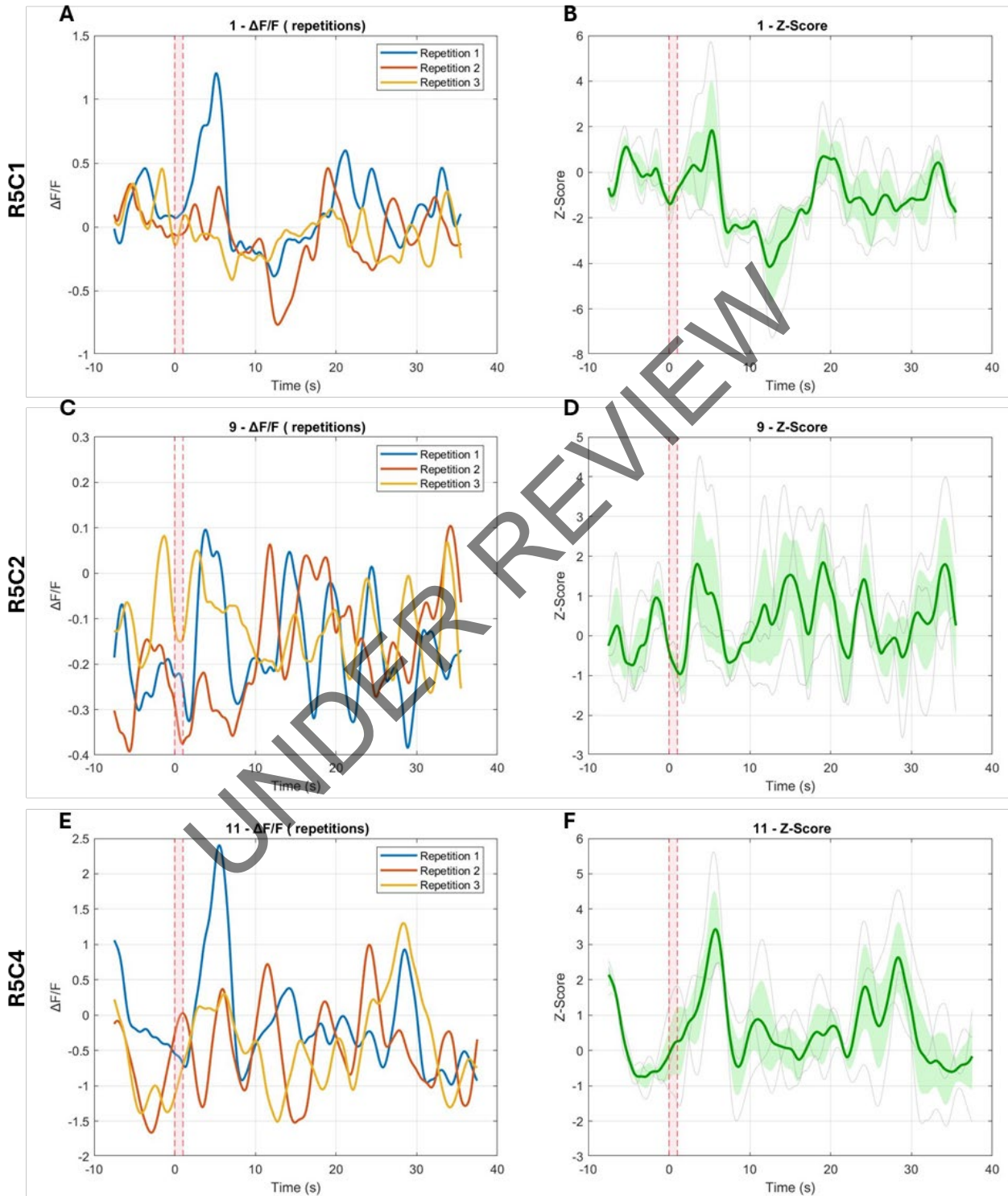


Figure 8 Delta F/F signal separated by stimulation repetition at one location with parameter set 1 in all 3 animals (A, C, E) Z-score normalized to 7 s pre-stimulation (B,D,F) The stimulation duration is marked in red.

Stimulation in awake animals was performed at multiple locations using parameters identical to those described in table 3. Figure 7 shows the $\Delta F/F$ results from one representative animal. The average $\Delta F/F$ over 3 stimulations are plotted in dark blue, the individual stimulations at each location are shown in grey, with the mean \pm SEM shown in light blue. A $\Delta F/F$ change associated with stimulation appears to occur at location 11, positioned +1 mm anterior and 0.6 mm lateral to the perpendicular stimulation site at 8 mm depth. These data were recorded in the animal implanted with chip R5C4, which showed a PNP of 0.29 MPa at 8 mm depth. The individual stimulation repetitions for this location are shown in Figure 8 E, illustrating that the observed effect is primarily driven by the first of the three stimulations. Figure 8 F shows the averaged z-score of these stimulations, normalized to the 7-second baseline before each stimulation.

Figure 8 A–D illustrates the same analysis for the most promising stimulation location for condition 1 in the other two recorded animals. For the animal implanted with chip R5C1, this was –1 mm anterior and –1 mm lateral, with a maximum peak negative pressure of 0.37 MPa. For the animal with chip R5C2, this location was +1 mm anterior and +1 mm lateral, with a peak negative pressure of 0.12 MPa. In all three animals, the first stimulation produced the largest response, and the animal with the lowest pressure profile showed the weakest Delta F/F change, but the stimulation-evoked effects are consistent with the other other stimulation responses when looking at the normalizes data.

Figure 9 further shows stimulation at 0/–0.6/8 mm in the animal with chip R5C4 using stimulation parameter 4. In this case, a potential response is visible during the first and second stimulations, but most clearly during the second. This may indicate a refractory period dependent on the stimulation parameters, during which subsequent stimulations evoke reduced or no dopamine release. If confirmed, this would imply that longer intervals between stimulations will be required in future experiments to avoid interference between repeated pulses.

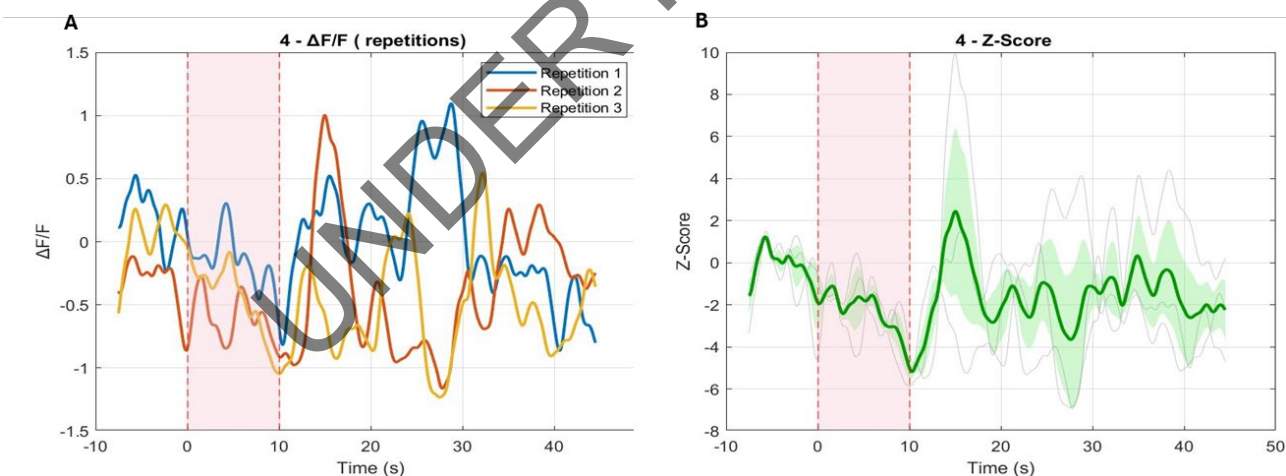


Figure 9 Stimulation of animal 1 with chip R5C4 at AP 0/ML -0.6/DV-8 mm with parameter set 4. The stimulation duration is marked in red.

Finally, the safety of repeated stimulations was assessed by examining microglial density at the stimulation site. An increase in microglia would suggest tissue damage or inflammation. Comparison of stimulated animals with a dummy-implanted control animal revealed no observable differences, indicating no detectable tissue damage with repeated stimulation with the tested parameters.

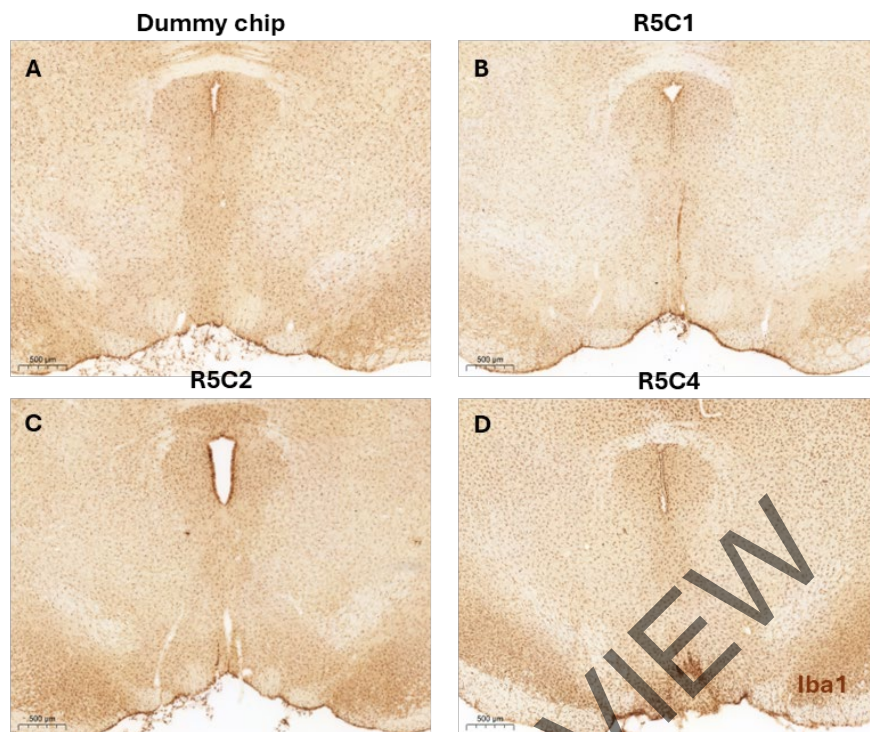


Figure 10 Iba 1 staining to check for tissue damage or inflammation at the stimulation site in an animal implanted with a Dummy chip (A), as well as the 3 real chips (B-D)

3. Conclusions

Report D4.4 presents on-going findings on the two key functionalities of the future EBI device: the first results from the *in vivo* use of the ECoG electrode grid designed for high spatial-temporal resolution *neural activity recording* (eREC) from the cortex; and the initial *in vivo* attempts to validate the *epidural focused ultrasound* system for steerable, multi-site neural stimulation (eFUS). At this point, the two functions are being assessed independently of each other, the functional integration of the eREC and the eFUS capacities will be reported on at a later time point in D4.5.

The 32 and 64-channel cortical grid electrodes were manufactured in Ghent and delivered to Freiburg for *in vivo* testing. For the study reported in this document, only the 64-channel electrodes were used. The grid electrodes were implanted on the midline of the cortex (covering cortical areas bilaterally), recording mainly from the Anterior Cingulate Cortex (Cg1), but likely picking up signals also from secondary Motor Cortex (M2). The cingulate cortex was targeted as it is part of the neural network associated with emotion/mood regulation, and the neuropathology of depression, and as such, a rational choice to attempt to identify electrophysiological biomarkers dissociating the FSL rodent depression model from the control animals. The FSLs spontaneously show depressive-like, including anxiety-like behaviours, and the introduction of the acute stress condition into the testing protocol aimed to exacerbate potential resting-state and event related changes in the recorded brain oscillations. The collected data was transferred to Newronika, who used the data to establish an analysis pipeline that integrates both linear and non-linear features to identify potential biomarkers from the ECoG recordings. A thorough assessment of the preliminary data can be read in their report D5.1. In short, the groups need to be expanded but initial analysis indicates that condition-dependent differences across the FSL and the control animals were noted both at the power spectral density and high beta and high gamma bands. The additional behavior and physiological assessment carried out on the animals confirmed a higher baseline, and a more blunted response to stress, in corticosterone levels in the FSL animals compared to the controls. The sample numbers used for the analysis in the changes in corticosterone levels are being increased, and a more accurate assessment will be included in an updated report. A follow-up report will also include more detailed analysis correlating individual animal's changes in electrophysiological parameters with their stress response as reflected in the changes in the corticosterone levels. Overall, the experience with the 64-channel ECoG electrode is positive: both the *in vivo* functioning and the data analysis pipeline have been validated, and we need to pursue the identification and biological meaning of the biomarkers.

Concerning the *in vivo* validation of the eFUS chip, we report steady, but slower than anticipated progress. Using the microbubble approach to study the *in vivo* effect of the eFUS stimulation confirms that perpendicular stimulation using the device is accurate, and the strongest signal was consistently observed at the stimulation location perpendicular to the center of the chip—the first position stimulated. Demonstrating “steerability” has been less clear, probably due to the limited half-life of microbubbles – these trials tend to be done at a later stage - and due to the decrease in focal pressure when the ultrasound beam is steered (deviates from the perpendicular target).

As described in previous reports from Freiburg, the studying of the *in vivo* physiological capacity of the eFUS chip was done in conjunction with fiber photometry that permits the monitoring of changes in specific neurotransmitters (in our case dopamine) in a high resolution spatial and temporal manner. The experience reported in the document is for the moment limited to three animals. The testing protocols need refinement, data assessment needs to be faster, and samples need to increase; nevertheless, there are positive take-aways. *In all three animals, we observed possible indications for stimulation effects on the dopamine release in the NAc.* Although this can only be confirmed with repetitive testing in the future which could unfortunately not be done in these first animals due to the loss of the implant or chip failure.

Nonetheless the possible effect could be seen in at least one stimulation site in all animals and higher peak $\Delta F/F$ values seem to correlate with the PNP of the chips at 8 mm. The proposed response seems to start at the end of stimulation, which could indicate a different stimulation dynamic compared to DBS. Steering the beam, produced different outcomes confirming that most likely different targets were stimulated. For example, the “best” target for the animal implanted with chip R5C1, was –1 mm anterior and –1 mm lateral from the predicted “best” target, obtained with a maximum PNP of 0.37 MPa. For the animal with chip R5C2, this location was +1 mm anterior and +1 mm lateral from the predicted “best” target, with a PNP of 0.12 MPa. Finally, the safety of repeated stimulations was assessed by examining microglial density at the stimulation site. An increase in microglia would suggest tissue damage or inflammation. Comparison of stimulated animals with a dummy-implanted control animal revealed no observable differences, indicating no detectable tissue damage with repeated stimulation with the tested parameters.

The “work in progress” nature of the on-going *in vivo* efforts are clearly demonstrated by the need to resolve emerging issues in order to pursue the validation. For example, the original connector with which the first chip came was not suitable for *in vivo*, longitudinal and repetitive recording as it detached too easily. The connector was replaced with a more suitable version that took into account the head position and increased head movement during the *in vivo* use in moving/ awake animals. The three eFUS chips tested so far had different technical profiles, for example, they differed in their max PNP ranging between 0.12 and 0.37 MPa. We also had a case of short circuiting which resulted in a malfunction and a revision of the chip-sealing method and rendering it more hermetic from the electrolytes it comes in contact with. Safety features need to be integrated into the chip design to deal with excessive heat (e.g. heat sink) or to automatically shut-off in case overheating is detected (e.g. maximum 1.5°C increase in the chip). Steps leading to reduction of heat generation would permit testing a wider range of stimulation parameters such as longer burst durations and higher duty cycles.

Additional issues that need(ed) to be dealt with are surgical and implantation related. The preparation for the *in vivo* and chronic testing of the eFUS chips requires multiple and relatively long surgical steps. For example, accurate neurotransmitter release using fiber photometry requires consistent placement of virus injection, and implantation of optic fiber. Even using stereotactic surgery (which increases precision), in a proportion of the animals, unavoidably, there will be inaccuracies as the surgery is based on estimating the coordinates from the “bregma”. Typically, the in-built inaccuracies are dealt by adjusting and increasing the sample numbers. Similarly in the current case, the validation of the physiological effects of the eFUS will need a much higher number than the three tested so far; we estimate that we will need to test *in vivo* at least 10-13 functioning eFUS chips to make headways.

Finally, perhaps the most crucial and sensitive surgical related issue that emerged is the position of the craniotomy, and the care required to avoid any damage to the central sinus. Any temporary, even partial disruption of blood flow through the central sinus has shown to result in brain swelling, which can impact on the animal’s vitality and extend or even compromise the animal’s post-surgical recovery. It is important to point out this is not directly related to the eFUS device itself, and is likely to be a species-specific issue, due to proportion of the required craniotomy (determined by the chip size) in relation to the skull.

In summary, the microbubble experience suggests that accurate/ predictable targeting is possible. We have developed a protocol permitting the chronic implantation of the eFUS chip for long-term *in vivo* testing, identifying critical steps in the multi-stage surgical protocol. We have put in place a parameter testing protocol and rapid data assessment using MATLAB script, which will permit more informed testing of “promising” parameters and sites. The on-going trouble-shooting/improvement of the eFUS chips and of the validation protocol will continue with increasing sample number of tested animals.

UPSIDE Website: <https://project-upside.eu>

Annex 1: MATLAB script

The MATLAB script used to analyse the fiber photometry data is available here:

<https://github.com/STX-UKF/UPSIDE.git>

UNDER REVIEW

4. References

1. Buzsáki, G. *Rhythms of the Brain*. (Oxford University Press, New York, 2006).
2. Buzsáki, G. & Vöröslakos, M. Brain rhythms have come of age. *Neuron* **111**, 922–926 (2023).
3. Boby, K. & Veerasingam, S. Depression diagnosis: EEG-based cognitive biomarkers and machine learning. *Behav Brain Res* **478**, 115325 (2025).
4. Steyn, S. F. An Updated Bio-Behavioral Profile of the Flinders Sensitive Line Rat: Reviewing the Findings of the Past Decade. *Pharmacol Res Perspect* **13**, e70058 (2025).
5. Thiele, S. *et al.* Long-term characterization of the Flinders Sensitive Line rodent model of human depression: Behavioral and PET evidence of a dysfunctional entorhinal cortex. *Behav. Brain Res.* **300**, 11–24 (2016).
6. Döbrössy, M. D. *et al.* Neuromodulation in Psychiatric disorders: Experimental and Clinical evidence for reward and motivation network Deep Brain Stimulation: Focus on the medial forebrain bundle. *Eur J Neurosci* **53**, 89–113 (2021).
7. Bruchim-Samuel, M. *et al.* Electrical stimulation of the vmPFC serves as a remote control to affect VTA activity and improve depressive-like behavior. *Exp Neurol* **283**, 255–263 (2016).
8. Gazit, T. *et al.* Programmed deep brain stimulation synchronizes VTA gamma band field potential and alleviates depressive-like behavior in rats. *Neuropharmacology* **91**, 135–141 (2015).
9. Overstreet, D. H. Modeling depression in animal models. *Methods Mol. Biol.* **829**, 125–144 (2012).
10. Voget, M. *et al.* Altered local field potential activity and serotonergic neurotransmission are further characteristics of the Flinders sensitive line rat model of depression. *Behav Brain Res* **291**, 299–305 (2015).
11. Bühning, F. *et al.* Electrophysiological and molecular effects of bilateral deep brain stimulation of the medial forebrain bundle in a rodent model of depression. *Exp Neurol* **355**, 114122 (2022).
12. Jenkinson, N. & Brown, P. New insights into the relationship between dopamine, beta oscillations and motor function. *Trends Neurosci* **34**, 611–618 (2011).
13. Chikermane, M. *et al.* Cortical beta oscillations map to shared brain networks modulated by dopamine. *eLife* **13**, RP97184 (2024).
14. Sporn, S., Hein, T. & Herrojo Ruiz, M. Alterations in the amplitude and burst rate of beta oscillations impair reward-dependent motor learning in anxiety. *eLife* **9**, e50654.
15. Xue, L. *et al.* Abnormal beta bursts of depression in the orbitofrontal cortex and its relationship with clinical symptoms. *Journal of Affective Disorders* **369**, 1168–1177 (2025).
16. Sabatini, B. L. & Tian, L. Imaging Neurotransmitter and Neuromodulator Dynamics In Vivo with Genetically Encoded Indicators. *Neuron* **108**, 17–32 (2020).
17. Wang, Y., DeMarco, E. M., Witzel, L. S. & Keighron, J. D. A selected review of recent advances in the study of neuronal circuits using fiber photometry. *Pharmacol Biochem Behav* **201**, 173113 (2021).
18. Wu, Z., Lin, D. & Li, Y. Pushing the frontiers: tools for monitoring neurotransmitters and neuromodulators. *Nat Rev Neurosci* **23**, 257–274 (2022).
19. Simpson, E. H. *et al.* Lights, fiber, action! A primer on in vivo fiber photometry. *Neuron* **112**, 718–739 (2024).
20. Ashouri Vajari, D. *et al.* Medial forebrain bundle DBS differentially modulates dopamine release in the nucleus accumbens in a rodent model of depression. *Exp Neurol* **327**, 113224 (2020).
21. Duan, Z., Zhao, W., Tong, Y., Coenen, V. A. & Döbrössy, M. D. Acute and chronic gene expression activation following medial forebrain bundle DBS and selective dopamine pathway stimulation. *Sci Rep* **15**, 7131 (2025).
22. Duan, Z., Tong, Y., Coenen, V. A. & Döbrössy, M. D. Deep brain stimulation of medial forebrain bundle modulates noradrenergic activity and feedforward inhibition in rodent model of depression. *Transl Psychiatry* **15**, 343 (2025).
23. Miguel Telega, L., Ashouri Vajari, D., Ramanathan, C., Coenen, V. A. & Döbrössy, M. D. Chronic in vivo sequelae of repetitive acute mfb-DBS on accumbal dopamine and midbrain neuronal activity. *J Neurochem* <https://doi.org/10.1111/jnc.16223> (2024) doi:10.1111/jnc.16223.
24. Miguel Telega, L., Ashouri Vajari, D., Stieglitz, T., Coenen, V. A. & Döbrössy, M. D. New Insights into In Vivo Dopamine Physiology and Neurostimulation: A Fiber Photometry Study Highlighting the Impact of Medial Forebrain Bundle Deep Brain Stimulation on the Nucleus Accumbens. *Brain Sci* **12**, 1105 (2022).
25. Ornelas, L. C. & Besheer, J. Predator Odor Stressor, 2,3,5-Trimethyl-3-Thiazoline (TMT): Assessment of Stress Reactive Behaviors During an Animal Model of Traumatic Stress in Rats. *Curr Protoc* **4**, e967 (2024).
26. Sun, F. *et al.* Next-generation GRAB sensors for monitoring dopaminergic activity in vivo. *Nat Methods* **17**, 1156–1166 (2020).